blood

Prepublished online March 17, 2014;
doi:10.1182/blood-2013-12-544569

Development and characterization of a physiologically relevant model of lymphocyte migration in chronic lymphocytic leukemia

Elisabeth Walsby, Andrea Buggins, Stephen Devereux, Ceri Jones, Guy Pratt, Paul Brennan, Chris Fegan and Chris Pepper

Blood (print ISSN 0006-4971, online ISSN 1528-0020), is published weekly by the American Society of Hematology, 2021 L St, NW, Suite 900, Washington DC 20036.

Blood First Edition Paper, prepublished online March 17, 2014; DOI 10.1182/blood-2013-12-544569

Development and characterization of a physiologically relevant model of lymphocyte migration in chronic lymphocytic leukemia

Elisabeth Walsby[1], Andrea Buggins[2], Stephen Devereux[2], Ceri Jones[1], Guy Pratt[3], Paul Brennan[1], Chris Fegan[1], Chris Pepper[1]

[1]Cardiff CLL Research Group, Institute of Cancer & Genetics, School of Medicine, Cardiff University, Heath Park, Cardiff, UK. [2]Department of Haematology, King's College London, London, UK. [3]CRUK Institute for Cancer Studies, University of Birmingham, Vincent Drive, Edgbaston, Birmingham, UK.

Corresponding author: Professor Chris Pepper, Cardiff CLL Research Group, Institute of Cancer & Genetics, School of Medicine, Cardiff University, Heath Park, Cardiff, UK, CF14 4XN.
Tel: +44 (0)2920687057, Fax: +44 (0)2920744655, email: peppercj@cf.ac.uk

Condensed title: Modeling CLL cell migration under shear

Keywords: CLL, shear force, endothelial cells, migration

Key points:

- We have developed a novel *in vitro* system to model how shear force and transient interaction with endothelial cells alter CLL cell phenotype and behavior.
- We have used our model to investigate CLL cell migration and determined the critical role for the integrin $\alpha 4\beta 1$ in this process.

Abstract

There is growing evidence that lymphocyte trafficking contributes to the clinical course of chronic lymphocytic leukemia (CLL) but to date only static *in vitro* cultures have been used to study these phenomena. To address this we have developed a dynamic *in vitro* model in which CLL cells experience shear forces equivalent to those in capillary beds and are made to flow through capillary-like hollow fibers lined with endothelial cells. CLL cells treated in this way increased their expression of CD62L, CXCR4 (both $P<0.0001$), CD49d and CD5 (both $P=0.003$) directly as a result of the shear force. Furthermore, CLL cells migrated through the endothelium into the 'extravascular' space (EVS) (mean migration: $1.37\% \pm 2.14\%$, $n=21$). Migrated CLL cells had significantly higher expression of CD49d ($P=0.02$), MMP-9 ($P=0.004$), CD38 ($P=0.009$), CD80 ($P=0.04$) and CD69 ($P=0.04$) compared with CLL cells that remained in the circulation. The degree of migration observed strongly correlated with CD49d expression ($r^2=0.47$, $P=0.01$) and treatment with the CD49d blocking antibody, Natalizumab resulted in significantly decreased migration ($P=0.01$). Taken together our data provide evidence for a novel, dynamic and tractable *in vitro* model of lymphocyte migration and confirm that CD49d is a critical regulator of this process in CLL.

Introduction

Chronic lymphocytic leukemia (CLL) is characterized by a clonal expansion of $CD5^+CD19^+$ B-cells found predominantly in the peripheral blood and lymphoid tissues. Although CLL is a proliferative disease[1], the majority of circulating CLL cells are arrested in G0/G1 of the cell cycle. Consequently the peripheral vasculature is often viewed as a passive transit zone, with very little known about the dynamics of tissue homing, migration and recirculation out of and into this microenvironment or the critical molecular interactions that drive these processes. To date, most *in vitro* studies of migration have been confined to static cultures using transwell plates, which are devoid of vascular shear force and the influence of endothelial cell interactions[2]. Shear stress on endothelial cells results in alignment and elongation of the cells, tight junction formation, decreased DNA synthesis and cell cycle arrest[3]. These limitations have become increasingly pertinent as there is growing evidence that trafficking to the microenvironmental niches of the bone marrow and lymph nodes affords cytoprotection to CLL cells[4]. Furthermore, in the lymph nodes, CLL cells interact with accessory cells including T-cells, stromal cells and endothelial cells resulting in the activation of NF-κB in the CLL cells[5,6], which promotes CLL cell proliferation[7-10]. Hence the predisposition of CLL cells to return to pro-survival, pro-proliferative tissues from the peripheral vasculature may be a critical factor in determining the clinical course of the disease. In keeping with this concept, gene expression profiling revealed that increased expression of genes that code for proteins involved in the control of cell movement were correlated with poor prognosis[11,12]. One such protein, CD49d, which interacts with VCAM-1 on endothelial cells during the process of CLL cell migration, has emerged as an important modulator of the pathology of CLL as evidenced by the fact that it is an independent prognostic marker in this disease[13-15].

Here we describe the development and characterization of a novel circulating model system designed to investigate the interactions of CLL cells and endothelial cells under physiologically relevant shear forces. Endothelial cells

were seeded into hollow fibers and subjected to shear in order to encourage the formation of pseudo-vessels. Subsequently CLL cells were circulated through the hollow fibers in order to mimic the transient contact with endothelial cells encountered in the capillary beds. Using this model system we demonstrated that shear induced a number of significant changes in endothelial cell and CLL cell phenotypes. In addition, we were able to demonstrate a time-dependent increase in CLL cell transendothelial migration, which was associated with the up-regulation of CD49d, MMP-9, CD38 and CD80 on CLL cells recovered from the 'extravascular' space. Targeted inhibition of CD49d, using an anti-CD49d blocking antibody, resulted in a significant reduction in the level of migration providing evidence for the key role this integrin plays in CLL cell migration.

Methods

Cells and patient characteristics

Peripheral blood samples were obtained from CLL patients attending outpatient clinics in accordance with the Declaration of Helsinki; ethical approval was obtained from the South East Wales Local Research Ethics Committee (LREC #02/4806). CLL PBMCs were isolated by density gradient centrifugation using Lymphoprep (Axis-Shield). The clinical characteristics of the patients are shown in Table 1.

Modifying a hollow fiber bioreactor

A hollow fiber bioreactor system (FiberCell Systems Inc) was adapted to generate an *in vitro* model of circulating CLL. The Bioreactor utilizes a peristaltic pump to create a flow of medium at a defined shear force (dynes/cm^2) through a closed system consisting of a reservoir of medium, wide tubing and a cartridge containing porous hollow fibers (Figure 1A). The FiberCell Systems Polysulfone Plus cartridge (C2025) hollow fibers were coated with matrix proteins to allow attachment of endothelial cells to the insides of the hollow fiber. The fibers in the cartridge were activated by 70% ethanol, followed by water and then gelatin (0.2% solution, Sigma Aldrich) was allowed to adhere to the insides of the hollow fibers for 2h. M199 medium (Sigma Aldrich) supplemented with 20% FBS (Life

Technologies) was used to gently wash unbound matrix protein from the hollow fibers and allow its removal from the system. In experiments where the hollow fibers were coated with endothelial cells, $15x10^6$ HUVEC (or HMEC-1) cells (Life Technologies) were introduced into the hollow fibers and allowed to adhere to the gelatin-coated fibers for an additional 2h. Non-adhered cells were then collected and removed from the system. The system was filled with 50ml M199 medium supplemented with 20% FBS and circulation initiated. Medium was circulated through the system with a shear force of 1.5 dynes/cm^2 overnight before the shear force was increased to 10 dynes/cm^2 for 6h before being decreased to 5 dynes/cm^2 for a minimum of 2h. Shear force was increased in these increments to encourage the HUVEC cells in the hollow fibers to form firm adhesion and to align along the fibers to form pseudo-vessels. CLL cells were subsequently introduced into the circulating system through port 2 of the cartridge (Figure 1A). At the point of introduction of CLL to the circulating system, recombinant human IL-4 (R&D Systems) was added to the medium at a final concentration of 5ng/ml.

Scanning electron microscopy

Cartridges were flushed with PBS to remove all medium then fixed for 24h in 2.5% v/v glutaraldehyde in PBS. Fixative was removed by washing twice with double distilled water for 5 minutes. An adapted version of the Progressive Lowering of Temperature protocol was employed[16,17]. Fibers were cut transversely and longitudinally, placed on self-adhesive carbon tape adhered to the surface of an aluminium stub and sputter coated with a gold target for 8 min in an EMscope sputter coater. Samples were viewed on a JEOL 840A scanning electron microscope (SEM) operating at 5kV and images recorded using SIS digital software.

Characterisation of endothelial cells pre- and post-circulation

HUVEC and HMEC-1 cells were removed from liquid culture or from the hollow fibers of the circulating system after 48h using an enzyme-free cell dissociation buffer (Life Technologies) and gentle agitation. Expression of ICAM-1 (BD),

PECAM-1 (R&D Systems), VCAM-1 and VEGFR2 (Life Technologies) were determined by flow cytometry.

Antibody labeling of CLL cells

CLL cells were circulated through the system for 1h before samples were removed from the circulating compartment (Figure 1A). CLL cells were then circulated for a further 48h before additional samples were removed. Following the retrieval of CLL cells from the circulating system the cells were labeled with fluorescence-tagged antibodies: CD19-Brilliant Violet-520, CD49d-PE-Cy7, CD38-Brilliant Violet-605, CD62L-eFluor450, CXCR4-PerCP-Cy5.5, CD80-PE, CD11a-APC, CD44-APC-Cy7, CD69-Alexa Fluor-700 (BioLegend), CD5-ECD (Beckman Coulter) and MMP-9-FITC (R&D Systems). Cells labeled with anti-MMP-9 antibody were fixed and permeabilized prior to labeling. Circulated CLL cells were compared to CLL cells prior to circulation and cells maintained in static culture conditions. Flow cytometry was performed on an Aria III FACS machine (Becton Dickinson) and data was analyzed using FlowJo software (Tree Star Inc.).

Migration

The FiberCell Systems Polysulfone Plus cartridges (C2025) are packed with hollow fibers with an internal radius of 350μM. The hollow fibers contain pores of ~0.2μM along their length (Figure 1A) to allow the exchange of medium (and potentially cells) with the 'extravascular' space (EVS). The EVS was accessed via port 3 in the cartridge (Figure 1A). Migration of CLL cells from the circulating system to the EVS was measured by collecting 100μl of circulating medium from the circulating compartment and from the EVS at 1h and 48h post introduction of CLL cells. These samples were analyzed by flow cytometry and the total number of live cells in 100μl sampled from each port was measured. The percentage of the circulating population that migrated was calculated according to the formula:

$$\% \text{ migration} = 100 \times (N_{P3}/(N_{P2} + N_{P3}))$$

N_{P2}=number of live cells in 100µl of sample from the circulating compartment

N_{P3}=number of live cells in 100µl of sample from the EVS

Separate samples from the circulating and EVS compartments of the model were labeled with the panel of antibodies detailed above and expression of the markers was compared on CLL cells recovered from the two compartments.

Polystyrene beads (unlabeled (10µm) beads (Beckman Coulter) or FITC-labeled (2.5µm) beads (Dako)) were added to the circulating system and circulated for 1h before samples were taken from the circulating and EVS compartments. These samples were analyzed by flow cytometry to determine whether the polystyrene beads could passively pass into the EVS.

Blocking CD49d functionality

Freshly isolated CLL cells were pre-treated (30 mins) with 20µg/10^6 CLL cells of the anti-CD49d antibody, Natalizumab (Elan Pharma International Ltd) prior to their introduction into the circulating system. In addition, untreated CLL cells from the same patient were introduced into a parallel cartridge. Untreated and Natalizumab-treated CLL cells were harvested from the circulating and extravascular compartments of each system after 1h and 48h. The level of CLL cell migration into the EVS in the presence and absence of Natalizumab at both time points was then calculated.

Results

Endothelial cells adhered to the inside of hollow fibers and aligned under shear force

The circulating model of CLL that we have developed is comprised of an adapted hollow fiber bioreactor with the interior of the hollow fibers lined with primary human umbilical vein endothelial (HUVEC) cells (Figure 1A and B). We also evaluated a microvascular endothelial cell line (HMEC-1) in order to compare and contrast the effects of different endothelium on CLL cell survival,

phenoptype and migratory capacity.[18,19] Under the peristaltic action of the pump in the bioreactor the HUVEC (or HMEC-1) cells were subjected to shear force (5 dynes/cm^2) equivalent to that present in the capillary beds[20]. Scanning electron microscopy (SEM) of the interior of the lined hollow fibers confirmed that the HUVEC cells under 5 dynes/cm^2 for 24h showed evidence of flattening and spreading along the inside surface of the hollow fiber (Figure 1C). However, we noted that short-term exposure to higher shear forces (10 dynes/cm^2 for 6h) encouraged further flattening and elongation and more complete coverage of the hollow fibers (Figure 1D). We therefore employed this strategy in subsequent experiments prior to reducing the shear forces to 5 dynes/cm^2 before the introduction of CLL cells into the model. As the hollow fibers are embedded in resin at the ends of the cartridges, the medium, containing CLL cells, could only circulate via the inside of the hollow fibers allowing interactions with endothelial cells under shear stress (Figure 1E).

Shear force induced an altered phenotype on endothelial cells

HUVEC and HMEC-1 cells recovered from the interior of the hollow fibers retained the expression of endothelial cell markers VCAM-1, PECAM-1, ICAM-1 and VEGFR2 but showed shear-induced reductions in all the markers when compared to cells grown in static cultures (Figure 1F and Figure S1 respectively). These data are consistent with previous reports showing that the expression of ICAM-1 and VCAM-1 are markedly decreased on endothelial cells placed under shear[21,22].

Transient interaction with endothelial cells maintained CLL cell viability

Although long-lived *in vivo*, CLL cells rapidly undergo apoptosis when cultured *in vitro*[23,24] unless they are supported by co-culture[25-27]. We have previously shown that static co-culture on endothelial cells provides cytoprotection for CLL cells[6,28] so we set out to establish whether transient interactions with endothelial cells under shear force could also maintain CLL cell viability. Figure 1G shows that there was no significant loss in CLL cell viability when the CLL cells were cultured in our HUVEC-lined circulating model system when compared with

static HUVEC co-culture. Similar results were obtained using HMEC-1-lined cartridges (Figure S1).

CLL cells increased their expression of CD62L, CXCR4, CD5 and CD49d as a result of circulation

CLL cells recovered from our circulating system showed a number of significant changes in phenotype when compared to baseline expression (time 0). After 48h in circulation CLL cells showed significantly increased expression of the selectin CD62L (Figure 2A, $P<0.0001$), the chemokine receptor CXCR4 (Figure 2B, $P<0.0001$), the negative regulator of BCR signaling, CD5 (Figure 2C, $P=0.003$), the adhesion molecule CD49d (Figure 2D, $P=0.004$) and the early activation antigen CD69 (Figure 2E, $P=0.007$). In contrast, no significant change in the expression of CD38, CD80, MMP-9 and CD19 was observed as a result of transient interaction with endothelial cells under shear (Figure 2F, G, H, I). Furthermore, experiments performed with the HMEC-1 cell line induced similar phenotypic changes (Figure S2).

CLL cells actively migrated into the 'extravascular' space

The ends of the hollow fibers in the circulating system are embedded in resin ensuring all cells flowing through the system pass through the lumen of the hollow fibers. Therefore no cells can passively leave the circulation and enter the space surrounding the hollow fibers (described here as the 'extravascular' space (EVS)). However, we consistently recovered CLL cells from the EVS even after just 1h of circulation (Figure 3A and Figure S3) and noted that the number of cells recovered was time-dependent (1h: 0.44% ±0.56; 48h: 1.37% ±2.14) Figure 3B shows that the percentage of migration was significantly increased after 48h ($P=0.03$). The hollow fibers are perforated along their entire length by a network of pores (~0.2μm) that could potentially facilitate the escape of CLL cells into the EVS. In order to establish whether objects approximately the size of CLL cells could be recovered from the EVS, we introduced polystyrene beads (10μm) into the system for 1h and then sampled 100μl of medium from the circulating and extravascular compartments (Figure 3Ci). Beads were readily recovered from the circulating compartment but no beads were recovered from the EVS. We next introduced smaller (2.5μm), fluorescent beads into the circulation system

(Figure 3Cii). Again, no beads were recovered from the EVS of the circulating system confirming that the beads were not able to passively move from the circulating compartment into the EVS. Therefore, the time-dependent recovery of CLL cells from the EVS indicated that these cells were actively migrating, rather than passively diffusing, out of the circulating compartment.

Migrated CLL cells had higher expression of MMP-9, CD49d, CD80, CD69 and CD38

CLL cells recovered from the EVS had a distinct phenotype when compared to paired samples recovered from the circulating compartment at the same time point. Migrated cells showed increased expression of the B-cell co-receptor CD19 (P=0.0008), the gelatinase MMP-9 (P=0.004), the adhesion molecule CD49d (P=0.02), the co-stimulatory molecule CD80 (P=0.04) and the activation marker CD69 (P=0.05) at 1h (Figure 3D). After 48h, expression of these markers was further increased on the migrated CLL cells (Figure 3E) and this was accompanied by significantly elevated expression of CD38 at this time point (P=0.009). Consistent with these findings, higher expression of CD38[29] and CD69[5] have been reported on CLL cells derived from tissue microenvironments. It is worthy of note that none of the changes in CLL cell phenotype were specific to HUVEC interactions as the HMEC-1 cell line also promoted CLL cell migration and induced very similar changes in phenotype (Figure S4).

CD49d expression correlated with CLL cell migration

CD49d expression on CLL cells that migrated into the EVS correlated with MMP-9 expression (Figure 4A, r^2=0.5, P<0.0001) and CD38 (Figure 4B, r^2=0.8, P<0.0001). These findings are in keeping with previous studies that showed that MMP-9 is regulated by CD49d[30] and is correlated with CD38[13,14]. In addition, CD38 expression correlated with MMP-9 expression (Figure 4C, r^2=0.5, P<0.0001) consistent with these molecules functioning in a macro-molecular complex and all being involved in trafficking of CLL cells into the protective microenvironments found in lymph nodes[31]. This was further supported by the correlation found between MMP-9 and CXCR4 (Figure 4D, r^2=0.2, P=0.025). CD49d expression on CLL cells has been previously associated with a worse

clinical prognosis[13,14,32]. Here we show for the first time that the expression of CD49d on circulating CLL cells correlates with the level of migration out of the circulation into the EVS (Figure 4E, r^2=0.4658, P=0.01). The relationship between all the other markers measured and migration are shown in Figure S5.

Inhibition of CD49d function with Natalizumab inhibited CLL cell migration

The correlation observed between CD49d expression and the migratory potential of CLL cells suggested that it might be a therapeutic target in CLL. Given that normal B-lymphocytes do not appear to require this integrin for transendothelial migration[33], blockade of $\alpha4\beta1$ may selectively inhibit CLL cell trafficking. The anti-CD49d antibody Natalizumab has been shown to prevent the interaction of CD49d and VCAM-1 on endothelial cells[34] so we assessed the effects of this antibody into our model system. The model can operate two separate cartridges in tandem, which allowed us to compare cells isolated from the same patient at the same time under different conditions. In one cartridge CLL cells were circulated without Natalizumab and in the other cartridge, CLL cells were pre-treated with Natalizumab for 30 minutes prior to introduction into the system. CLL cells treated with Natalizumab showed a significant decrease in their ability to migrate out of circulation into the EVS after 48h (Figure 4F, P=0.01).

Normal PBMCs showed similar phenotypic changes and migrate in our circulating model

In order to determine whether our findings were restricted to CLL lymphocytes, we introduced PBMC's from four healthy donors in our dynamic model system. Normal B-cells were identified by the expression of CD19 and T-cells were identified as $CD5^+/CD19^-$, cells recovered from the circulating compartment and the EVS. Circulating normal B-cells showed significant increases in CD62L (Figure 5A) and CXCR4 expression (Figure 5B, normal B- and T-cells). No significant differences were seen in CD5 expression in normal B- or T-cells over 48h in circulation (Figure 5C). In addition, we showed time-dependent increases in CD49d and CD69 in normal B-cells recovered from the circulation but these were not significant (Figure 5D and 5E). Furthermore, both normal B- and T-cells

migrated into the EVS (Figure 5F). Consistent with our findings with CLL B-cells, CD19 expression was increased on normal B-cells that migrated compared with B-cells in circulation (P=0.016, Figure 5G). In contrast to CLL B-cells, normal B- and T-cells showed significantly decreased expression of CD49d and CD69 in cells that migrated into the EVS (Figure 5G). In addition, small but non-significant increases in MMP-9 and CD80 expression were observed on normal B-cells that migrated into the EVS. The lack of induction of both CD49d and CD38 in migrated normal B-cells when compared to CLL B-cells is consistent with these molecules being important in the survival of CLL cells[32] and previous reports have shown that CD49d is essential for CLL cell migration but not normal B-cell migration[33,35]. Despite these apparent molecular differences, we found no significant difference in B-cell migration in normal and CLL samples at 1h (P=0.31). However, at 48h a higher percentage of CLL B-cells migrated compared with B-cells from normal samples (CLL: 1.37%±2.14, normal B-cells 0.32%±0.05, P=0.03, Figure 5H).

Discussion

Despite advances in our knowledge of the pathology of CLL there are still significant gaps in our understanding of the key mechanisms that modulate the clinical course of this heterogenous disease. There is a growing appreciation that the complex interactions between CLL cells and their microenvironments hold the key to improving clinical outcomes in this disease. This is perhaps best exemplified by the success of the Bruton's tyrosine kinase (BTK) inhibitor ibrutinib[36]. Although the molecular target of this agent is clear, its profound effects on ejecting CLL cells from the lymphoid tissues was unexpected. This in turn has reinforced the importance of tissue homing and retention within pro-survival, pro-proliferative sites as pathological drivers in CLL. It is therefore important to dissect the key molecular events that underpin these processes in order to explain the variation in the natural pathology of this disease and develop more rational therapeutic strategies.

None of the existing *in vitro* co-culture systems of CLL provide an accurate proxy for the peripheral vasculature of CLL patients and hence cannot provide

meaningful insights into the process of extravasation and migration. In order to address this, we have developed a dynamic model system in which CLL cells were circulated through endothelium-lined hollow fibers under shear forces comparable to those present in the capillary beds and high endothelial venules[37]. Under these conditions we showed that HUVEC cells flattened against the walls of the hollow fibers and form pseudo-vessels. They also took on the phenotype of endothelial cells under shear[21,22]. Shear force promotes tight junction formation between HUVEC endothelial cells[38] and is required for peripheral blood lymphocyte adhesion to[39] and migration across the endothelium[40].

Next we characterized the effects of introducing CLL cells into our hollow fiber system. CLL cell viability was maintained at levels equivalent to that achieved in static co-culture with endothelial cells. Furthermore, circulation of CLL cells in our system induced specific phenotypic changes; the extent of these changes was sample-dependent implying that some CLL cells are more predisposed to responding to the co-stimuli of shear and transient interaction with endothelial cells. The changes that were induced were consistent with priming of CLL cells for migration; we observed an early increase in the expression of the selectin CD62L as well as increased expression of CD49d, CXCR4, CD5 and CD69. CD62L is necessary for the initially tethering of the lymphocytes to endothelial cells via its ligand, PNAd[41] and CD49d which is necessary for CLL cell adhesion to endothelial cell walls[32]. In addition, circulating CLL cells also showed a significant increase in the expression of CXCR4, the receptor of SDF-1, which has chemotactic activity for lymphocytes and results in homing to protective microenvironments[42]. CD69 has been shown to be a strong predictor of CLL prognosis and to be up regulated by microenvironmental contact[5,11]. The increase in expression of these markers on CLL cells under shear force implicating the action of shear force in the control of expression of these regulators of CLL cell motility.

Consistent with these phenotypic changes, we were able to demonstrate that CLL cells underwent transendothelial migration into the EVS of our model system. The accumulation of CLL cells in the EVS was associated with higher expression

of MMP-9, CD38, CD49d, CD80 and CD69. Previous reports have indicated that these molecules may physically interact[31] and CD38 and CD49d are associated with worse prognosis in CLL[14] and lymph node infiltration[8,32]. Furthermore, correlations between CD38 and CD49d expression has previously been reported[43] as have interactions between CD38, CD49d and MMP-9[31] and CXCR4[10]. In addition, interactions between CD49d on the CLL and VCAM-1 on endothelial cells are crucial for the adhesion of CLL cells to stromal cells[44] and in stroma-mediated protection from apoptosis[45]. The level of migration in our circulating system was strongly associated with the expression of CD49d on the circulating CLL cells. This is consistent with the concept that CD49d is a critical regulator of CLL cell migration[33,37] and may explain its prognostic impact on CLL patients[15]. We therefore set out to inhibit the function of this integrin by using the blocking antibody Natalizumab. Pre-treatment of CLL cells with Natalizumab resulted in reduced migratory ability in our model system highlighting the importance of CD49d to CLL cell homing and migration. However, we were not able to abolish CLL cell migration under these conditions suggesting that either the inhibition of CD49d was incomplete or that other molecules also modulate the capacity of CLL cells to migrate in our system. These possibilities are not mutually exclusive and we are currently evaluating of the role of other key molecular targets using multiple inhibition strategies.

Finally, we established that our model system could also be used to investigate the behavior of non-malignant lymphocytes. In keeping with our CLL cell data, normal B-cells and T-cells showed phenotypic evidence of activation when they were recovered from the circulating compartment of our system. Subsequently, both lymphocyte subsets were recovered from the EVS suggesting that our model system is suitable for investigating normal lymphocyte transendothelial migration.

In summary, we have built and characterized a dynamic *in vitro* model system of the peripheral vasculature that is suitable for investigating the key molecular drivers of transendothelial migration. In the context of CLL, this represents a significant advance as it provides a physiologically relevant means of

understanding how CLL cells interact with and traffic across endothelial cell barriers. It is also ideally suited to the study the effects of new therapeutic agents targeting molecules involved in lymphocyte migration and homing.

Acknowledgements

This work was supported in part by Leukaemia and Lymphoma Research and the Leukaemia Research Appeal for Wales. The authors wish to thank Jan Hobot for his expert assistance with all electron microscopy undertaken in the preparation of this manuscript and John Cadwell for interesting discussions about the adaptation of the bioreactor.

Authorship contributions

EW carried out the experimental work, analyzed the data and wrote the manuscript. AB carried out the experimental work, analyzed the data and revised the manuscript. SD provided clinical samples, analyzed data and revised the manuscript. CJ provided clinical samples, analyzed data and revised the manuscript. GP provided clinical samples, analyzed data and revised the manuscript. PB analyzed data and revised the manuscript. CF provided clinical samples and data and revised the manuscript. CP conceived the work and revised the manuscript.

Disclosure of Interests

None of the authors have any conflicts of interest to disclose.

References

1. Messmer BT, Messmer D, Allen SL, et al. In vivo measurements document the dynamic cellular kinetics of chronic lymphocytic leukemia B cells. *J Clin Invest*. 2005;115(3):755-764.
2. Chan PY, Aruffo A. VLA-4 integrin mediates lymphocyte migration on the inducible endothelial cell ligand VCAM-1 and the extracellular matrix ligand fibronectin. *J Biol Chem*. 1993;268(33):24655-24664.
3. Akimoto S, Mitsumata M, Sasaguri T, Yoshida Y. Laminar shear stress inhibits vascular endothelial cell proliferation by inducing cyclin-dependent kinase inhibitor p21(Sdi1/Cip1/Waf1). *Circ Res*. 2000;86(2):185-190.
4. Burger JA, Burkle A. The CXCR4 chemokine receptor in acute and chronic leukaemia: a marrow homing receptor and potential therapeutic target. *Br J Haematol*. 2007;137(4):288-296.
5. Herishanu Y, Perez-Galan P, Liu D, et al. The lymph node microenvironment promotes B-cell receptor signaling, NF-kappaB activation, and tumor proliferation in chronic lymphocytic leukemia. *Blood*. 2011;117(2):563-574.
6. Buggins AG, Pepper C, Patten PE, et al. Interaction with vascular endothelium enhances survival in primary chronic lymphocytic leukemia cells via NF-kappaB activation and de novo gene transcription. *Cancer Res*. 2010;70(19):7523-7533.
7. Patten PE, Buggins AG, Richards J, et al. CD38 expression in chronic lymphocytic leukemia is regulated by the tumor microenvironment. *Blood*. 2008;111(10):5173-5181.
8. Deaglio S, Malavasi F. Chronic lymphocytic leukemia microenvironment: shifting the balance from apoptosis to proliferation. *Haematologica*. 2009;94(6):752-756.
9. Granziero L, Ghia P, Circosta P, et al. Survivin is expressed on CD40 stimulation and interfaces proliferation and apoptosis in B-cell chronic lymphocytic leukemia. *Blood*. 2001;97(9):2777-2783.
10. Vaisitti T. CD38 increases CXCL12-mediated signlas and homing of chronic lymphocytic leukemia cells. *Leukemia*. 2010;24(5):958-969.
11. Stamatopoulos B, Haibe-Kains B, Equeter C, et al. Gene expression profiling reveals differences in microenvironment interaction between patients with chronic lymphocytic leukemia expressing high versus low ZAP70 mRNA. *Haematologica*. 2009;94(6):790-799.
12. Deaglio S, Vaisitti T, Aydin S, et al. CD38 and ZAP-70 are functionally linked and mark CLL cells with high migratory potential. *Blood*. 2007;110(12):4012-4021.
13. Majid A, Lin TT, Best G, et al. CD49d is an independent prognostic marker that is associated with CXCR4 expression in CLL. *Leukemia research*. 2011;35(6):750-756.
14. Gattei V, Bulian P, Del Principe MI, et al. Relevance of CD49d protein expression as overall survival and progressive disease prognosticator in chronic lymphocytic leukemia. *Blood*. 2008;111(2):865-873.
15. Bulian P, Shanafelt TD, Fegan C, et al. CD49d Is the Strongest Flow Cytometry-Based Predictor of Overall Survival in Chronic Lymphocytic Leukemia. *J Clin Oncol*. 2014.

16. Newman GR, Hobot, J.A. Resin Microscopy and On-Section Immunocytochemistry (ed 2): Springer Verlag; 2001.
17. Walker M, Hobot JA, Newman GR, Bowler PG. Scanning electron microscopic examination of bacterial immobilisation in a carboxymethyl cellulose (AQUACEL) and alginate dressings. *Biomaterials*. 2003;24(5):883-890.
18. Ades EW, Candal FJ, Swerlick RA, et al. HMEC-1: establishment of an immortalized human microvascular endothelial cell line. *J Invest Dermatol*. 1992;99(6):683-690.
19. Schweitzer KM, Vicart P, Delouis C, et al. Characterization of a newly established human bone marrow endothelial cell line: distinct adhesive properties for hematopoietic progenitors compared with human umbilical vein endothelial cells. *Lab Invest*. 1997;76(1):25-36.
20. Cucullo L, Hossain M, Tierney W, Janigro D. A new dynamic in vitro modular capillaries-venules modular system: cerebrovascular physiology in a box. *BMC Neurosci*. 2013;14:18.
21. Ando J, Yamamoto K. Vascular mechanobiology: endothelial cell responses to fluid shear stress. *Circ J*. 2009;73(11):1983-1992.
22. Chiu JJ, Chen LJ, Lee PL, et al. Shear stress inhibits adhesion molecule expression in vascular endothelial cells induced by coculture with smooth muscle cells. *Blood*. 2003;101(7):2667-2674.
23. Pedersen IM, Kitada S, Leoni LM, et al. Protection of CLL B cells by a follicular dendritic cell line is dependent on induction of Mcl-1. *Blood*. 2002;100(5):1795-1801.
24. Burger JA, Tsukada N, Burger M, Zvaifler NJ, Dell'Aquila M, Kipps TJ. Blood-derived nurse-like cells protect chronic lymphocytic leukemia B cells from spontaneous apoptosis through stromal cell-derived factor-1. *Blood*. 2000;96(8):2655-2663.
25. Willimott S, Baou M, Huf S, Deaglio S, Wagner SD. Regulation of CD38 in proliferating chronic lymphocytic leukemia cells stimulated with CD154 and interleukin-4. *Haematologica*. 2007;92(10):1359-1366.
26. Edelmann J, Klein-Hitpass L, Carpinteiro A, et al. Bone marrow fibroblasts induce expression of PI3K/NF-kappaB pathway genes and a pro-angiogenic phenotype in CLL cells. *Leuk Res*. 2008;32(10):1565-1572.
27. Balakrishnan K, Burger JA, Wierda WG, Gandhi V. AT-101 induces apoptosis in CLL B cells and overcomes stromal cell-mediated Mcl-1 induction and drug resistance. *Blood*. 2009;113(1):149-153.
28. Hamilton E, Pearce L, Morgan L, et al. Mimicking the tumour microenvironment: three different co-culture systems induce a similar phenotype but distinct proliferative signals in primary chronic lymphocytic leukaemia cells. *British journal of haematology*. 2012;158(5):589-599.
29. Jaksic O. CD38 on B-cell chronic lymphocytic leukemia cells has higher expression in lymph nodes than in the peripheral blood or bone marrow. *Blood*. 2004;103(5):1968-1969.
30. Redondo-Munoz J, Escobar-Diaz E, Samaniego R, Terol MJ, Garcia-Marco JA, Garcia-Pardo A. MMP-9 in B-cell chronic lymphocytic leukemia is up-regulated by alpha4beta1 integrin or CXCR4 engagement via distinct signaling pathways, localizes to podosomes, and is involved in cell invasion and migration. *Blood*. 2006;108(9):3143-3151.

31. Buggins AG, Levi A, Gohil S, et al. Evidence for a macromolecular complex in poor prognosis CLL that contains CD38, CD49d, CD44 and MMP-9. *British journal of haematology*. 2011;154(2):216-222.
32. Zucchetto A, Benedetti D, Tripodo C, et al. CD38/CD31, the CCL3 and CCL4 chemokines, and CD49d/vascular cell adhesion molecule-1 are interchained by sequential events sustaining chronic lymphocytic leukemia cell survival. *Cancer Res*. 2009;69(9):4001-4009.
33. Till KJ, Spiller DG, Harris RJ, Chen H, Zuzel M, Cawley JC. CLL, but not normal, B cells are dependent on autocrine VEGF and alpha4beta1 integrin for chemokine-induced motility on and through endothelium. *Blood*. 2005;105(12):4813-4819.
34. Lesesve JF, Debouverie M, Decarvalho Bittencourt M, Bene MC. CD49d blockade by natalizumab therapy in patients with multiple sclerosis increases immature B-lymphocytes. *Bone Marrow Transplant*. 2011;46(11):1489-1491.
35. Worthylake RA, Burridge K. Leukocyte transendothelial migration: orchestrating the underlying molecular machinery. *Curr Opin Cell Biol*. 2001;13(5):569-577.
36. Byrd JC, Furman RR, Coutre SE, et al. Targeting BTK with ibrutinib in relapsed chronic lymphocytic leukemia. *N Engl J Med*. 2013;369(1):32-42.
37. Till KJ, Lin K, Zuzel M, Cawley JC. The chemokine receptor CCR7 and alpha4 integrin are important for migration of chronic lymphocytic leukemia cells into lymph nodes. *Blood*. 2002;99(8):2977-2984.
38. Burns AR, Walker DC, Brown ES, et al. Neutrophil transendothelial migration is independent of tight junctions and occurs preferentially at tricellular corners. *J Immunol*. 1997;159(6):2893-2903.
39. Woolf E, Grigorova I, Sagiv A, et al. Lymph node chemokines promote sustained T lymphocyte motility without triggering stable integrin adhesiveness in the absence of shear forces. *Nat Immunol*. 2007;8(10):1076-1085.
40. Cinamon G, Shinder V, Alon R. Shear forces promote lymphocyte migration across vascular endothelium bearing apical chemokines. *Nat Immunol*. 2001;2(6):515-522.
41. Alon R, Chen S, Puri KD, Finger EB, Springer TA. The kinetics of L-selectin tethers and the mechanics of selectin-mediated rolling. *J Cell Biol*. 1997;138(5):1169-1180.
42. Burger M, Hartmann T, Krome M, et al. Small peptide inhibitors of the CXCR4 chemokine receptor (CD184) antagonize the activation, migration, and antiapoptotic responses of CXCL12 in chronic lymphocytic leukemia B cells. *Blood*. 2005;106(5):1824-1830.
43. Redondo-Munoz J, Ugarte-Berzal E, Garcia-Marco JA, et al. Alpha4beta1 integrin and 190-kDa CD44v constitute a cell surface docking complex for gelatinase B/MMP-9 in chronic leukemic but not in normal B cells. *Blood*. 2008;112(1):169-178.
44. Munk Pedersen I, Reed J. Microenvironmental interactions and survival of CLL B-cells. *Leuk Lymphoma*. 2004;45(12):2365-2372.
45. Buchner M, Baer C, Prinz G, et al. Spleen tyrosine kinase inhibition prevents chemokine- and integrin-mediated stromal protective effects in chronic lymphocytic leukemia. *Blood*. 2010;115(22):4497-4506.

Table 1. Patient characteristics. Table showing the clinical characteristics of the 45 patients used in this study.

Factor	Subset	Number
Median Age		67 years
Range		29 - 85 years
Median Follow-up		6.2 years
Required treatment	Treated	19
	Untreated	26
Binet stage	A	39
	B/C	6
LDT (months)	>12	25
	<12	6
	Not determined	14
CD38 expression	<20%	26
	≥20%	19
	Not Determined	0
Genetics	Normal	5
	13q-	12
	12+	2
	$11q^-$ / $17p^-$	2
	Not Determined	24
IGHV Status	<98%	15
	≥98%	9
	Not Determined	21

LDT: Lymphocyte doubling time <12 months/ >12 months
CD38 expression: <20%/≥20% of the CLL B-cells expressing the antigen
IGHV status: ≥98% sequence homology with the closest germline sequence; <98% sequence homology with the closest germline sequence
Normal: No detectable cytogenetic aberration by FISH; 13q-: abnormalities involving loss of chromosome 13q; 12+: trisomy 12; $11q^-$ and $17p^-$: any FISH or karyotypic abnormality involving chromosome 11q or 17p

Figure Legends

Figure 1. Development of a novel circulating model of CLL (A) HUVEC cells were seeded into the hollow fibers of the bioreactor and exposed to physiologically relevant shear forces. Medium containing CLL cells was pumped around the system permitting transient interaction with the endothelial layer. The hollow fibers in the bioreactor have pores through which CLL cells can migrate into the space outside fibers; the extravascular space is shown in the cross sectional image of the cartridge. CLL cells were recovered from the circulating compartment and the extravascular space of the system via the access ports. (B) Photograph of the adapted bioreactor. (C) Scanning electron micrograph (SEM) of HUVEC cells on the interior of the hollow fibers after 5h of alignment at 5 dynes/cm^2. The beginning of flattening and spreading of the cells is visible. (D) SEM of HUVEC cells inside a hollow fiber following 6h alignment under 10 dynes/cm^2 followed by 24h at 5 dynes/cm^2. The HUVEC cells showed increased spreading and flattened resulting in coverage of the interior of the hollow fiber. (E) SEM of a transverse section of a lined hollow fiber showing the wall of the fiber with CLL cells visible in the inside of the fiber. Scale bars indicate 10 microns in all SEM images. (F) Expression of endothelial cell markers was measured by flow cytometry on HUVEC cells grown in both non-circulating static tissue culture flasks and on cells recovered from the hollow fibers after alignment under shear force. Expression of VCAM-1 (P=0.01), PECAM-1 (P=0.002) and VEGFR2 (P=0.05) were reduced in HUVEC cells under shear force. (G) CLL cell viability in circulating and static co-culture with HUVEC cells. There was no significant difference between CLL viability in circulating culture and in static co-culture with HUVEC cells. All culture conditions were supplemented with IL-4 (5ng/ml).

Figure 2. CLL cells circulating under physiologically relevant shear force showed increased expression of CD62L, CXCR4, CD5, CD49d and CD69

CLL cells were circulated through the circulating system with hollow fibers lined with HUVEC cells for 48h. Cell surface expression of (A) CD62L, (B) CXCR4, (C) CD5, (D) CD49d, (E) CD69, (F) CD38, (G) CD80, (H) MMP-9 and (I) CD19 was

measured by flow cytometry gated on doublet discriminated, lymphocytes represented as mean fluorescence intensity (MFI) values (** P<0.0001, * P<0.05).

Figure 3. CLL cells actively underwent transendothelial cell migration associated with the up-regulation of MMP-9, CD49d, CD80, CD38 and CD69

CLL cells were circulated through the hollow fiber model system lined with HUVEC endothelial cells for 48h. Paired samples were taken from the circulating compartment of the model and from the extravascular space. (A) SEM of the outside of a hollow fiber showing CLL cells that migrated from the inside of the fiber to the outside. Scale bar indicates 10 microns. (B) CLL cells showed a significant increase in migration at 48h when compared to 1h (n = 21, P=0.03). (C) Polystyrene beads were introduced into the circulating compartment of the circulating system and circulated for 1h. Aliquots of 100µl were removed from both the circulating and extravascular compartment and the number of beads in each 100µl aliquot were measured by flow cytometry. (Ci) 10µm beads and (Cii) 2.5µm fluorescent beads in the circulating compartment and below the dashed line in the extravascular compartment after 1h. No beads were recovered from the extravascular space in each of the three replicates of the experiment. In contrast, CLL cells were consistently recovered from the extravascular compartment at this time point. Compared with CLL cells remaining in the circulating compartment, CLL cells recovered from the extravascular space had increased expression of MMP-9, CD49d, CD80, CD38, CD69 and CD19 when measured by flow cytometry after (D) 1h and (E) 48h circulation around the system. Error bars indicate ±1S.D. around the mean fluorescence intensity on a population of doublet discriminated, $CD19^+$ lymphocytes. * P<0.05.

Figure 4. CLL cell migration correlated with CD49d expression and was inhibited by the CD49d antagonist Natalizumab

CLL cells that had been circulated in a closed system containing hollow fibers lined with HUVEC cells were recovered from both the circulating compartment and the extravascular compartment. CD49d expression correlated with (A) MMP-9 (r^2 = 0.5, n = 28) and (B) CD38 (r^2 = 0.8, n = 27). In addition, (C) MMP-9 and CD38 expression correlated with each other (r^2 = 0.5, n = 25) and (D) MMP-9

and CXCR4 expression levels correlated with each other (r^2 = 0.2, n=24). (E) CD49d expression on circulating CLL cells after 48h showed the strongest correlation with the percentage of migration of CLL cells into the extravascular space (r^2 = 0.47, n = 12). (F) In order to establish a functional role for CD49d in CLL cell migration, CLL cells were pre-treated with the anti-CD49d monoclonal antibody and then introduced into the circulating system. Natalizumab-treated CLL cells showed a significant reduction in their capacity to migrate into the extravascular space at 48h.

Figure 5. Normal B- and T-cells showed similar phenotypic changes when compared with CLL cells

PBMCs from four normal healthy donors were introduced into the circulating model in the same way as CLL PBMCs. Samples were then taken from the circulating compartment and the extravascular space at 48h and labeled with the same panel of cell surface markers used for the CLL samples. B-cells were identified as $CD19^+$ and T-cells as $CD5^+/CD19^-$. Expression (MFI) of (A) CD62L, (B) CXCR4, (C) CD5, (D) CD49d and (E) CD69 in circulating B-cells and T-cells is shown. (F) Normal B- and T-cells also migrated into the extravascular space and the percentage of B-cell and T-cell migration is shown (G) Expression of MMP-9, CD49d, CD80, CD38, CD69 and CD19 in normal B- and T-cells was compared in cells recovered from the extravascular space and cells remaining in the circulation compartment. (H) B-cells from normal samples migrated significantly less than CLL B-cells at 48h. Error bars indicate ±S.D., * $P<0.05$.

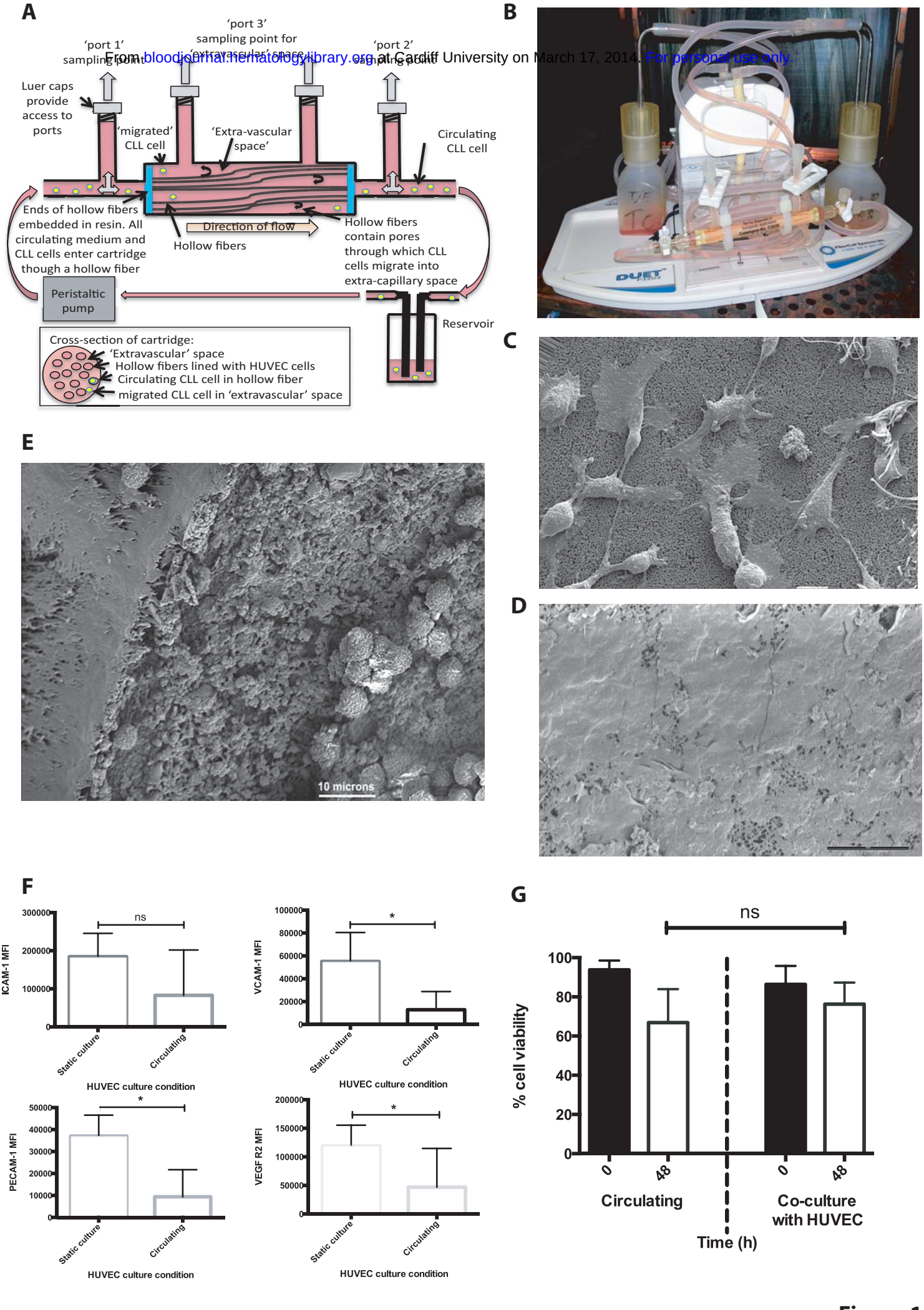

Figure 1

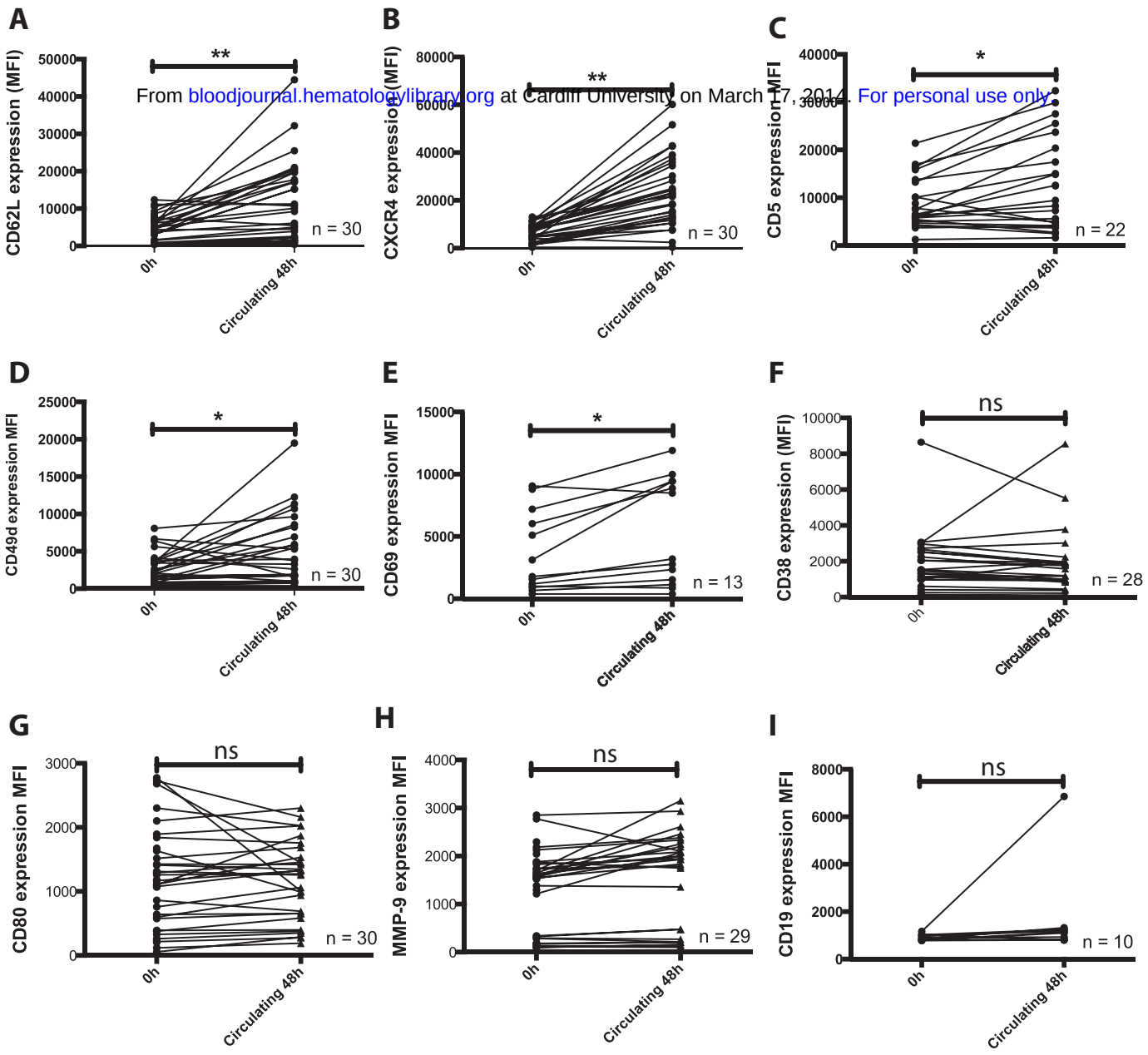

Figure 2

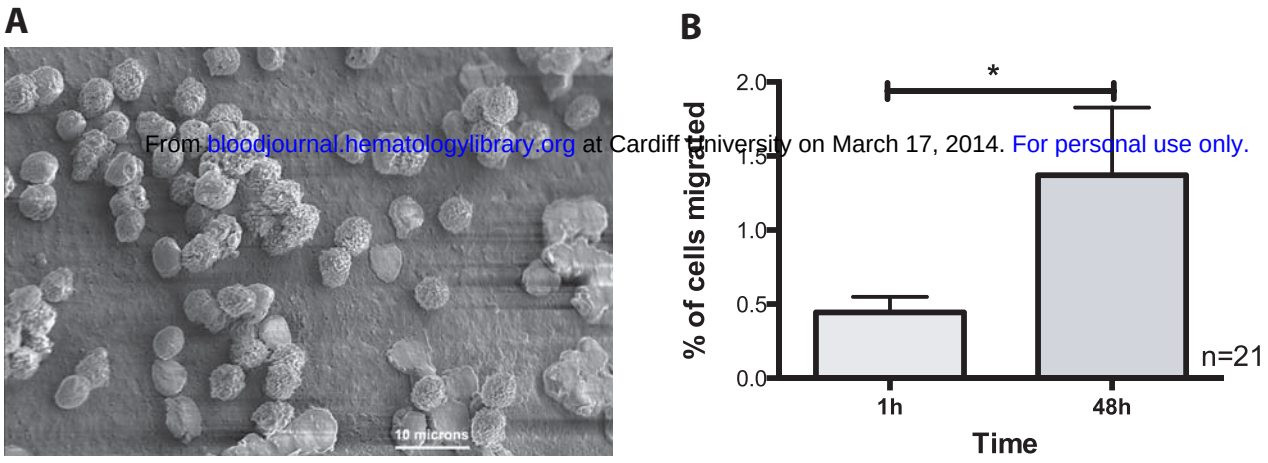

Figure 3

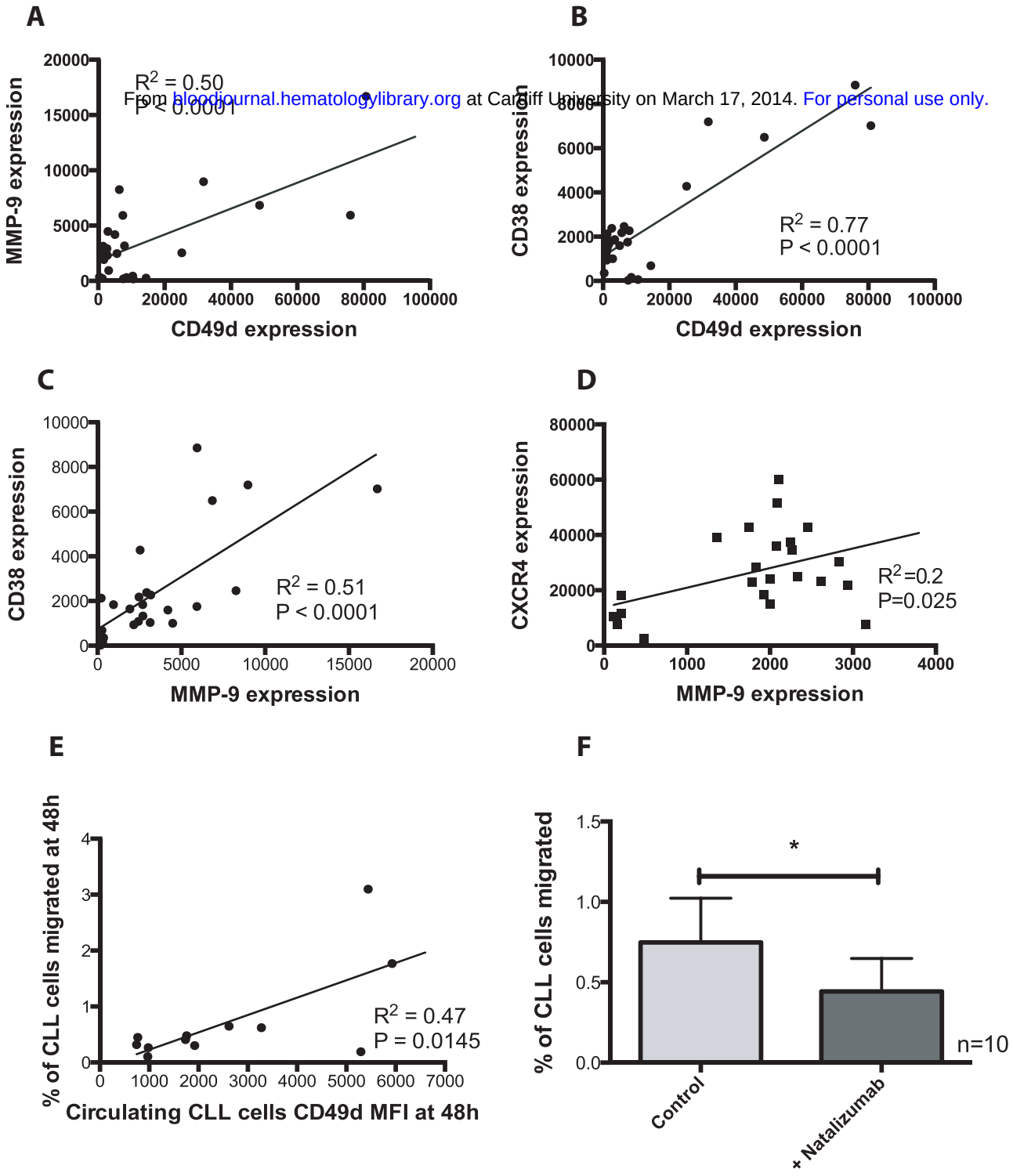

Figure 4

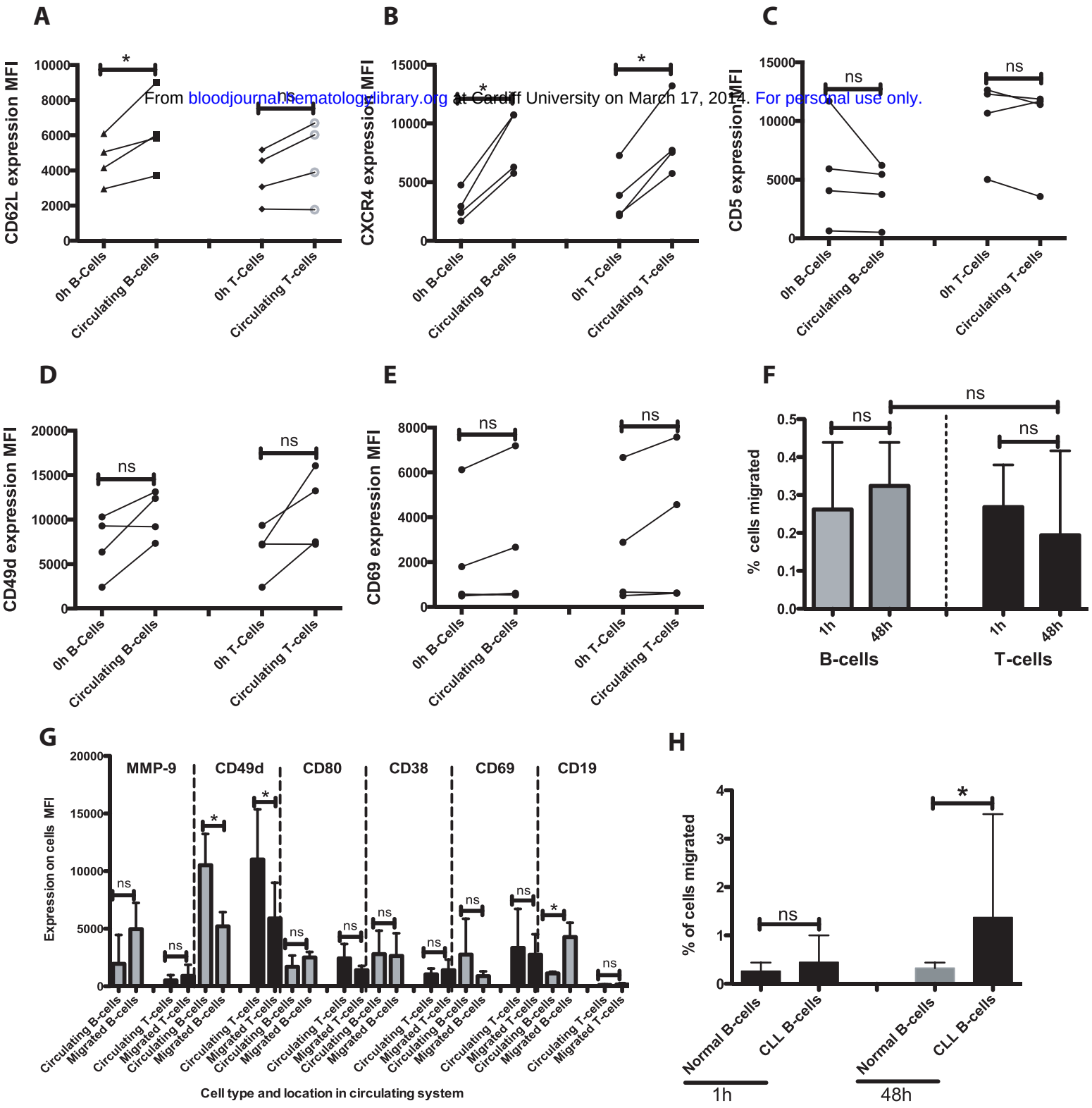

Figure 5